

THE EFFECT OF SWIRLING NUMBER VARIATION ON TURBULENT TRANSPORT AND MIXING PROCESSES IN SWIRLING RECIRCULATING FLOWS: EXPERIMENTAL AND NUMERICAL INVESTIGATIONS

C. Schneider, S. Repp, A. Sadiki, A. Dreizler, J. Janicka

Department of Mechanical Engineering, Darmstadt University of Technology
Petersenstr. 30, 64287 Darmstadt
ekt@hrzpub.tu-darmstadt.de

ABSTRACT

In this work, confined swirling reactive as well as non-reactive recirculating flows are analyzed experimentally and numerically. Extensive turbulent flow field measurements for the determination of the velocity components and the Reynolds stresses using 2D-Laser-Doppler Velocimetry are presented. In addition, selected results of Raman measurements for the simultaneous determination of temperature, mixture fraction and major species concentrations performed by Meier et al. (2000) at an identical set-up are included for a complete comparison of scalar as well as flow fields to numerical calculations based on RANS-modelling approach. Such results can be used to improve the understanding of the effects of swirl number variation on relevant transport and mixing processes and to provide an outstanding data base for subsequent development and validation of turbulence, mixing and turbulence-chemistry interaction models.

INTRODUCTION

Two major objectives in modern design of technical combustion systems, in which heat release and species transfer play a central role, are optimisation of combustion efficiency and reduction of pollutants. In order to optimize the description and prediction of flow and scalar transfer for such purposes, physicochemical combustion models need to be validated with measured data from experimental configurations of practical importance.

With regard to design efforts, by adjusting the swirl intensity it is possible to improve the mixing quality of the flow and to influence or to control physicochemical processes.

These characteristics provide the possibility to yield zones with specified equivalence ratio and thermal conditions in case of swirling flames. Characterized by recirculation of hot combustion products along with strong chemistry-effects, swirling confined reacting flows belong to the important and challenging tasks in modern CFD and laser diagnostics.

Swirling flows are generally classified into weak and strong cases depending on the swirl number intensity. Investigations on swirl number effects are rare. Caldas et al. (1995) report on investigations in unconfined configurations with and without swirl. Other work is focussed on swirling flames with a fixed swirl number either in unconfined configurations (e.g. Beltagui et al. (1993), Durao et al. (1991)) or in confined configurations (e.g. Altgeld et al. (1983), Heitor et al. (1992), Kremer (1998)).

With regard to numerical investigations, Reynolds stress closures are now commonly used in a variety of applications of complex turbulent flows. Concerning turbulent reacting flows, one needs various models to describe the turbulent fluid flow, the chemistry, thermodynamics, turbulence-chemistry interaction and radiation. A successful prediction depends on these models and on the numerical procedures used. However, the turbulence-chemistry interaction is of special importance regarding swirling flames. Different approaches to describe the non-linear nature of turbulence-chemistry interaction can be found in the literature (Pope (1985)). All approaches use turbulent combustion models which make use of statistical properties of the scalar field. The numerical analysis presented accounts for the turbulence-chemistry interaction by using a presumed probability density function or by applying the Monte-Carlo method.

Recently, Landefeld (1999) presented results for a confined configuration employing a swirl number of $S=0.9$ and using a multidimensional presumed-pdf. A comparison to a non-reacting case was not provided. Hinz (2000) investigated the same configuration by using the Monte Carlo pdf-method. Repp et al. (2000) analyzed in the same configuration the effects of turbulence-chemistry interaction modelling on the prediction of flow and scalar fields by comparing pdf-methods.

In this work, a presumed-pdf will be considered as coupling model to predict the effects of swirling number variation on turbulent transport and mixing

processes in swirling recirculating flows. The turbulence is modelled by using linear second order moment closures following Landefeld (1999), while the chemical reactions are described by the ILDM-method (Maas and Pope (1992)). Because the effect of combustion is obvious, we focus the numerical investigation on the reacting case by comparing the result to experimental data for different swirling numbers obtained by means of 2D-Laser Doppler Velocimetry and spontaneous raman spectroscopy.

FLOW CONFIGURATION AND EXPERIMENTAL SETUP

Measurements of the three mean velocity components, respective turbulence intensities and the Reynolds stresses have been carried out in an axisymmetric swirling recirculating flow using the swirling flame configuration presented in Fig.1 (TECFLAM burner). The flow is initialized by a swirl burner with moveable block consisting of a central bluff body, an inner annulus (inner diameter: 20 mm; outer diameter: 26 mm ($b=3$ mm)) for fuel gas exit and an outer annulus (inner diameter: 30 mm; outer diameter: $d=60$ mm) for swirling air. The swirl intensity is adjustable between the swirl number $S=0$ and $S=2$.

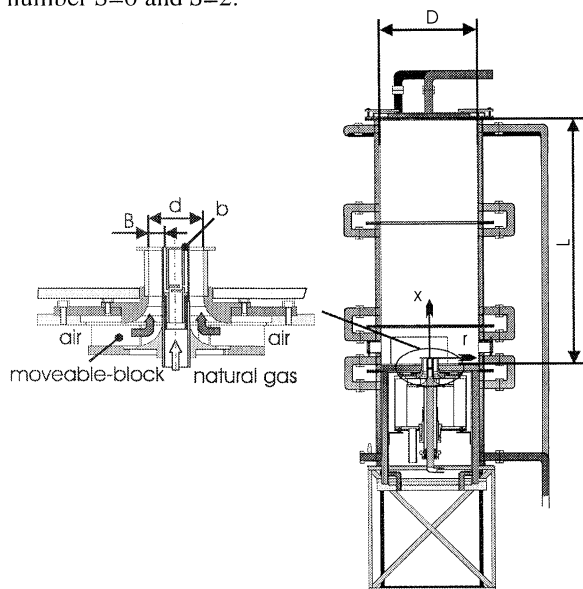


Figure 1 : TECFLAM swirl burner throat geometry and experimental setup.

The exhaust gas exits the combustion chamber (Fig.1, $L=1200$ mm, $D=500$ mm) at the top through an annulus of 15 mm width. The outlet is centrally blocked to prevent inflow of ambient air. With the thermal load of 150 kW this confined flow represents an application close to practical combustion systems.

Four different configurations were studied by changing the swirl number from $S=0.9$ to $S=1.4$ and investigating the flow with and without combustion.

| | | S09iso | S14iso | S09hot | S14hot |
|------------|---------------------|--------|--------|--------|--------|
| $S_{0,th}$ | [-] | 0.9 | 1.4 | 0.9 | 1.4 |
| P | [kW] | - | - | 150 | 150 |
| λ | [-] | 1.2 | 1.2 | 1.2 | 1.2 |
| Q_{gas} | [m ³ /h] | 15.9 | 15.9 | 15.9 | 15.9 |
| Q_{air} | [m ³ /h] | 174 | 174 | 174 | 174 |
| Re_{gas} | [-] | 5400 | 5400 | 7900 | 7900 |
| Re_{air} | [-] | 42900 | 42900 | 42900 | 42900 |

Table 1 : Boundary conditions for investigated configurations.

The case without combustion was accomplished by replacing the natural gas flow by a mixture of air and helium in order to guarantee similar conditions of the central outflow in terms of velocity and density at the burner head. The inner flow had a bulk velocity of 21 m/s representing a Reynolds number of $Re=7900$ for the natural gas and $Re=5400$ for the air/helium mixture. The airflow had a bulk velocity of 23 m/s resulting in a Reynolds number of 42900.

The LDV-measurements were carried out with a two-component fiber optic Laser-Doppler Velocimeter. The laser beam of a 4W argon ion laser was divided by means of a Bragg cell into two beam pairs with wavelengths of 514.5 nm and 488 nm, respectively. By use of a front lens with a focal length of 500 mm the measurement volume can be described as a cylinder with a diameter of 94 μ m and a length of 780 μ m. An estimate of the statistical error concerning the mean velocity is 6%, whereas fluctuations are accurate within 8%.

For reactive conditions, the determination of the species concentration and the temperature was carried out by using spontaneous raman scattering as described in detail in Meier et al. (2000). A flashlamp pumped dye laser was used to generate a 2 μ s long pulse at 489 nm with an energy of 3J. The spatial resolution was given by the beam width of 0.6mm at the focus in the chamber. The Raman signals were collected by photomultiplier tubes and were used to determine the main species concentrations, the mixture fraction and the density. By use of the main species concentration the temperature was obtained employing the ideal gas law. The accuracy achieved for the mean values is typically 2-3% for the temperature, 2% for N_2 , 4% for CO_2 and increases for smaller mole fractions. The accuracy of a single-pulse measurement was reduced due to photon statistics and was on the order

of 5% for the temperature, 5-7% for H₂O (with a mole fraction of 0.2 at 2000K), 12-15% for O₂ (mole fraction 0.03, T≈2000K), and 2% for CH₄ (mole fraction 1, T≈1000K).

MODELLING AND NUMERICAL SETUP

To describe the flow- and mixing field second order turbulence models of Jones and Musonge (1988) in its revised form (1994) is used. The density-velocity fluctuation is modelled with the well established assumption of Jones (1979) and the model of Daly and Harlow (1970) is applied for the unknown turbulent transport terms in the transport equation of the Reynolds stress components. For details see Repp et al. (2000).

Numerical results are obtained with a two-dimensional elliptic CFD code based on a staggered orthogonal grid and cylindrical coordinates. Assuming axisymmetry, the half plane of the combustion chamber is discretised by a 90 x 80 points grid condensed near the burner and the wall in axial and radial direction, respectively. Numerical methods applied are a QUICK scheme providing second order accuracy for discretisation of the convective terms and a time relaxation scheme in order to achieve stationary solutions. Pressure correction is performed using the SIMPLE algorithm.

Initial and boundary conditions

Inlet profiles are derived from the LDV measurements at an axial plane $x=1$ mm downstream of the burner throttle and adjusted such that correct volumetric flow rates of fuel and air are assured. Calculation results can be sensitive to the inlet boundary values, particularly with respect to the dissipation rate, which cannot be directly measured. Though the inlet profile of the dissipation rate can be determined from the given mean velocity and the profile of the turbulent kinetic energy, with an assumption of zero axial derivative, it is modelled here with a Prandtl mixing length l proportional to the annulus width R to give $\epsilon=C_{\mu}^{3/4} k^{3/2}/l$ with $l=R/C$, C to be determined. In our calculations, the value $C=5$ for the fuel is used. Standard wall functions are applied assuming the logarithmic law in the boundary layer. Only the reacting case with different swirling numbers will be numerically performed here.

The flame can be characterised by very intensive mixing and combustion processes in the near field of the nozzle. In the reaction zone, chemical kinetic effects are significant and the temperature is moderate. Hence, radiation is neglected. As test calculations have shown, radiation effects are of minor importance in the reaction zone near the burner. The simulations are then carried out under adiabatic conditions, thus neglecting convective and

radiative heat losses across the wall. For the accurate prediction of temperature profiles far downstream, this simplification can certainly not be applied.

RESULTS, DISCUSSION AND CONCLUSION

Flow field: Results of turbulent flow field measurements are presented in Figure 2 and 3 for two horizontal planes (10 mm and 90 mm) downstream of the burner head. Open symbols represent the isothermal case without combustion while closed symbols represent the reactive case. The results reveal a strong influence of the combustion on the flow characteristics particularly for axial positions of 90mm. In fact, an analysis of the Navier- Stokes equation shows that apart from density variations combustion modifies the viscosity through the dependence of the kinematic viscosity ν on the temperature. Because of $\nu \propto T^{3/2}$, the local turbulent Reynolds number is strongly dependent on the temperature. This effect cannot be neglected in combustion, as shown in Figures 2 and 3. Here, the reinforcement of the turbulence by the combustion is unequivocal. This effect is enhanced by increasing the swirl number from 0.9 to 1.4.

As depicted in Figure 2 and Figure 3, the maximum value of the mean axial velocity increases in the reacting case. The same is true for radial as well as tangential velocity components (not shown). This behaviour is due to the lowered density and the conservation of axial and angular momentum and agrees with the observation of Beltagui (1993). In addition, the length of the recirculation zone decreases in the reactive case, while its width broadens. By increasing the swirling number similar effects are observed.

The distribution of the shear stresses $\overline{u'w'}$ shows maximum values coincident with those of the rms of the axial velocity, with increasing values for the reacting flows and high swirl number. The same can be noticed for $\overline{u'v'}$ and of the rms of the radial velocity (not shown).

Figure 4 and Figure 5 show in more detail the flow field as measured for the reacting case. Data are plotted at 10 and 30 mm above the burner head for swirl numbers of 0.9 and 1.4. In comparison, results from RANS calculations are added to the figure. In general a promising agreement is found. For the higher swirl number the recirculation zone is wider and more pronounced as obvious from axial velocity profiles shown at the bottom of figure 4. Higher radial as well as tangential velocities are observed for increasing swirl. These findings are in good agreement to the numerical predictions. Especially for a swirl number of 1.4 there is observed a good agreement for the width of the mixing layer as indicated by the profiles of the turbulent kinetic energy \bar{k} .

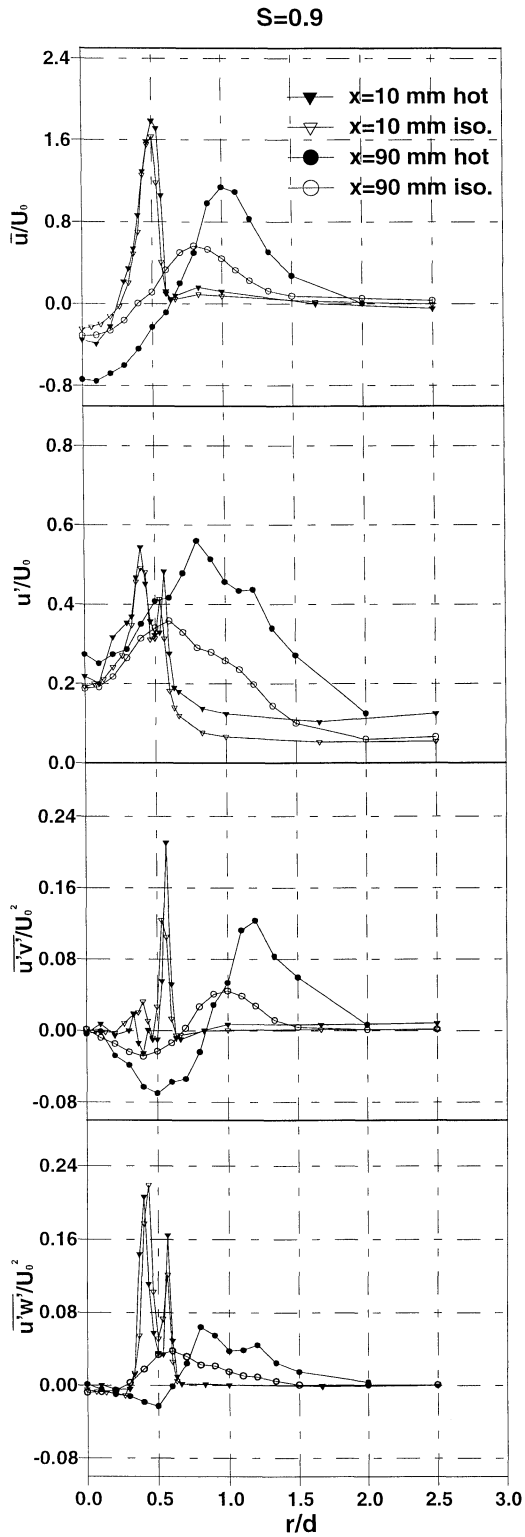


Figure 2 : Radial profiles of mean axial velocity \bar{u} , the rms of the axial velocity $\sqrt{u'^2}$, shear stress $\overline{u'v'}$ and shear stress $\overline{u'w'}$ in the planes $x=10$ mm and $x=90$ mm for $S=0.9$ normalised with the exit bulk velocity $U_0 = 23$ m/s.

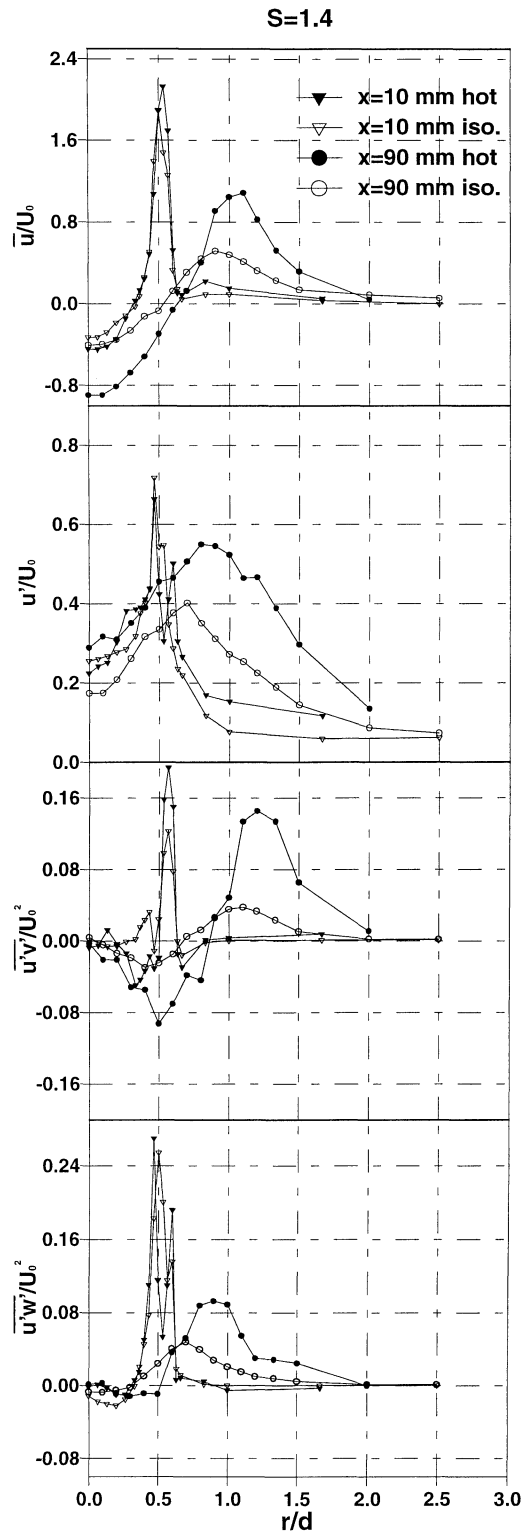


Figure 3 : Radial profiles of mean axial velocity \bar{u} , the rms of the axial velocity $\sqrt{u'^2}$, shear stress $\overline{u'v'}$ and shear stress $\overline{u'w'}$ in the planes $x=10$ mm and $x=90$ mm for $S=1.4$ normalised with the exit bulk velocity $U_0 = 23$ m/s.

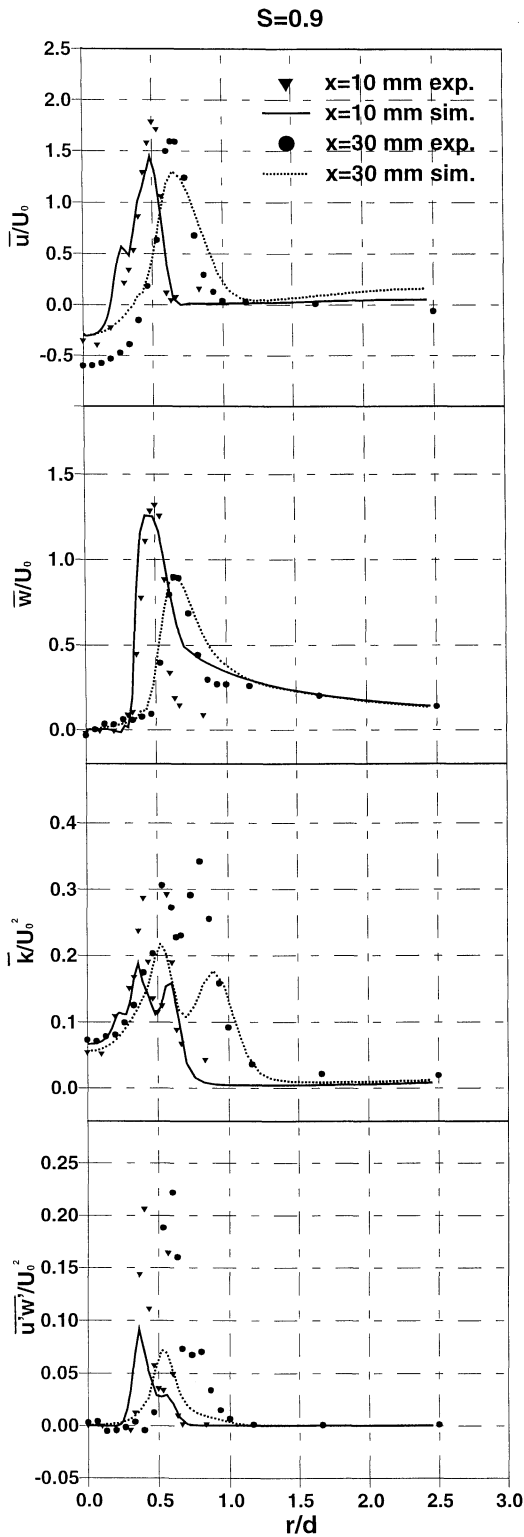


Figure 4 : Radial profiles of mean axial velocity \bar{u} , mean tangential velocity \bar{w} , turbulent kinetic energy \bar{k} and shear stress $\overline{u'w'}$ in the planes $x=10$ mm and $x=30$ mm for $S=0.9$ normalised with the exit bulk velocity $U_0 = 23$ m/s.

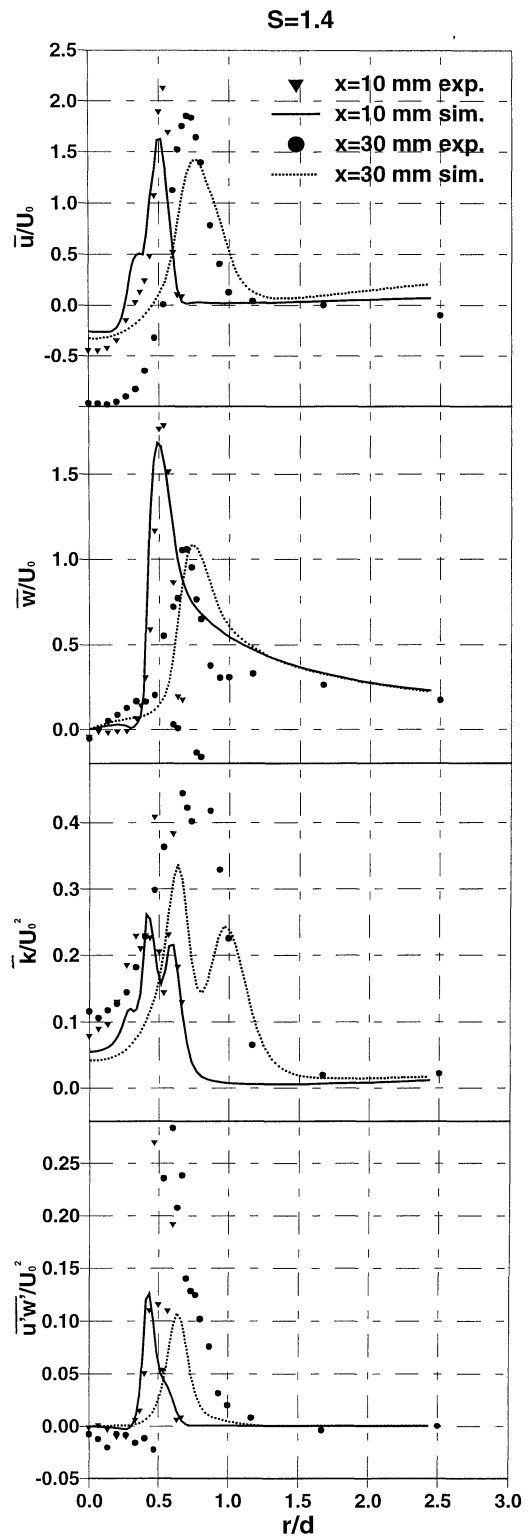


Figure 5 : Radial profiles of mean axial velocity \bar{u} , mean tangential velocity \bar{w} , turbulent kinetic energy \bar{k} and shear stress $\overline{u'w'}$ in the planes $x=10$ mm and $x=30$ mm for $S=1.4$ normalised with the exit bulk velocity $U_0 = 23$ m/s.

Scalar field: In Figure 6 distributions of species are shown at the axial positions $x=10\text{mm}$ and $x=40\text{mm}$. For the mean mixture fraction \bar{f} and its rms the profiles show \bar{f} being overpredicted at $x=40\text{mm}$ in the inner mixing layer. This tendency is confirmed by increasing the swirl number in which case the mixing is increased in general. This leads to the homogenisation of species distributions, what is one of the main objectives in designing technical applications. A similar picture is revealed for the mean and rms- data of the mass fraction of CO_2 . In general the profiles of scalar distribution obtained by numerical simulations are in good agreement with the experiment.

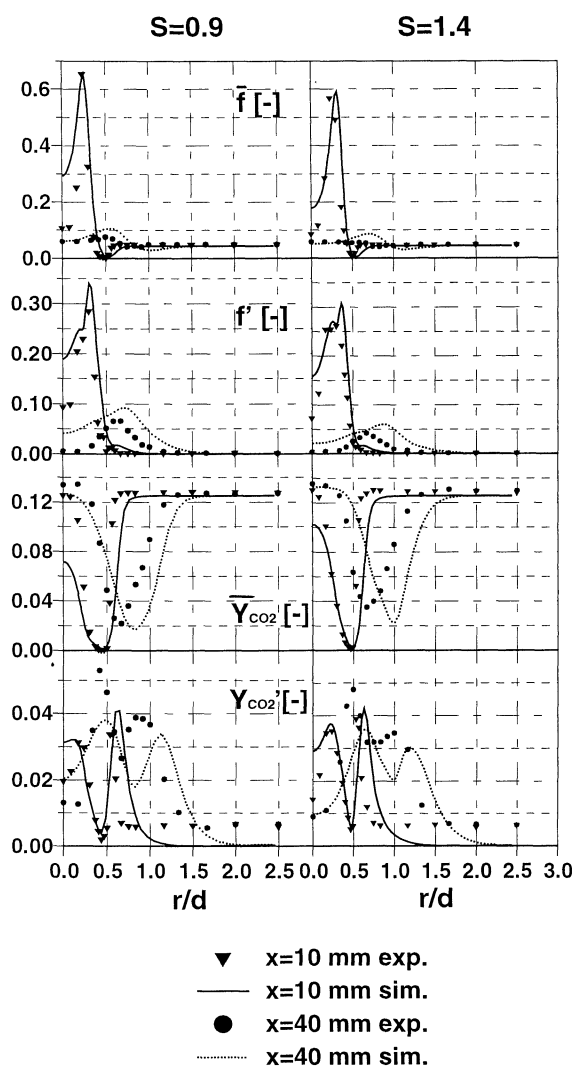


Figure 6 : Radial profiles of mean and the rms values of mixture fraction and mass fraction Y_{CO_2} in the planes $x=10\text{mm}$ and $x=40\text{mm}$.

ACKNOWLEDGEMENT

This work was supported by DFG (Deutsche Forschung Gemeinschaft) through SFB 568 (project B1 and B3). We gratefully acknowledge W. Meier for providing his raman data shown in Figure 6.

REFERENCES

- Altgeld, H., Jones, W.P., Wilhelmi, J. 1983: "Velocity Measurements in a Confined Swirl Driven Recirculating Flow", *Experiments in Fluids*, 1, 73-78.
- Beltagui, S.A., Kenbar, A.M.A., Maccallum, N.R.L. 1993: "Comparison of Measured Isothermal and Combusting Confined Swirling Flows: Peripheral Fuel Injection", *Exp. Thermal and Fluid Sci.*, Vol. 6, 147-156
- Caldas, F., Duarte, D., Ferrao, P., Heitor, M. V. 1995: "On the Effect of Swirl in a Turbulent Recirculating Flow", *ASME Fluids End. And Laser Anemom. Conf. And Exhib.*, Hilton Head, South Carolina, 95-100
- Durao, D.F.G., Heitor, M.V., Moreira, A.L.N. 1991: "Turbulent Transport Processes in Swirling Recirculating Non-Premixed Flames", 8th Symp. On Turbulent Shear Flows, München, 3151-3156
- Heitor, M. V., Moreira, A.L.N. 1992: "Velocity Characteristics of a Swirling Recirculating Flow", *Exp. Thermal and Fluid Science*, Vol. 5, pp. 369-380
- Hinz, A. 2000: "Numerische Simulation turbulenter Methandiffusionsflammen mittels Monter Carlo PDF Methoden", PhD-Thesis, TU Darmstadt.
- Kremer, A. 1998: "Turbulente Transportprozesse in Erdgas-Drallflammen unter Einfluß verschiedener Randbedingungen", PhD-Thesis, TU Darmstadt.
- Landenfeld, T. 1999: "Numerische Beschreibung turb. Methandiffusionsflammen mit Schließungsmodellen zweiter Ordnung und ang. Wahrscheinlichkeitsdichtefunktionen", PhD-Thesis, TU Darmstadt.
- Landenfeld, T., Kremer, A., Hassel, E.P., Janicka, J., Schäfer, T., Kazenwadel, J., Wolfrum, J. 1998: "Laser-diagnostic and Numerical Study of Strongly Swirling Natural Gas Flames", 28th Symp. on Combustion/The Combustion Institute.
- Maas, U., Pope, S.B. 1992: "Simplifying Chemical Kinetics: Intrinsic Low-Dimensional Manifolds in Composition Space", *Combustion and Flame*, 88:239-264.
- Meier, W., Keck, O., Noll, B., Kunz, O., Stricker, W. 2000: "Investigations in the TECFLAM Swirling Diffusion Flame: Laser Raman Measurements and CFD Calculations", *Appl. Phys. B* 71, 725-731.
- Pope, S. B. 1985: "PDF Methods for Turbulent Reacting Flows", *Progress in Energy and Science Combustion*.
- Repp, S., Sadiki, A., Schneider, C., Hinz, A., Landenfeld, T., Janicka, J., 2000: "Effects of Turbulence-Chemistry Interaction of the Prediction of Flow and Scalar Fields in Swirling Confined Reacting Flows: Comparison of PDF Methods", submitted to *Intern. Journal of Heat and Mass Transfer*.